Chymotrypsin Adsorption on Montmorillonite: Enzymatic Activity and Kinetic FTIR Structural Analysis

M.H. H Baron, M. Revault, S. Servagent-Noinville, J. Abadie, H. Quiquampoix

Journal of Colloid and Interface Science 214 (1999) 319-332.
DOI : 10.1006/jcis.1999.6189

Chymotrypsin Adsorption on Montmorillonite :

Enzymatic Activity and Kinetic FTIR Structural Analysis

M. H. Baron*[1], M. Revault[1], S. Servagent-Noinville[1], J. Abadie[2] and H. Quiquampoix[2]

[1]*Laboratoire de Dynamique, Interactions et Réactivité UPR 1580 CNRS-UNIVERSITE PARIS VI, 2 rue Henri Dunant, 94320 Thiais, France; and* [2]*UFR de Science du Sol INRA-ENSAM, 2 place Pierre Viala, 34060 Montpellier, France.*

Abbreviated title: Chymotrypsin Adsorption on Montmorillonite

---

To whom the correspondence should be addressed.

Dr M. H. Baron, Laboratoire de Dynamique, Interactions et Réactivité,

CNRS, 2 rue Henri Dunant, 94320-Thiais, France

Telephone : 00 33 1 49 78 11 15

Fax : 00 33 1 49 78 13 23

E mail : baron_mh@glvt-cnrs.fr

Journal of Colloid and Interface Science 214 (1999) 319-332.
DOI : 10.1006/jcis.1999.6189

Abstract

Soils have a large solid surface area and high adsorptive capacities. To determine if structural and solvation changes induced by adsorption on clays are related to changes in enzyme activity, α-chymotrypsin adsorbed on a phyllosilicate with an electronegative surface (montmorillonite) has been studied by transmission FTIR-spectroscopy. A comparison of the pH-dependent structural changes for the solution and adsorbed states probes the electrostatic origin of the adsorption. In the pD range 4.5-10, adsorption only perturbs some peripheral domains of the protein compared to the solution. Secondary structure unfolding affects about 15-20 peptide units. Parts of these domains become hydrated and others entail some self-association. However, the inactivation of the catalytic activity of the adsorbed enzyme in the 5-7 pD range is due less to these structural changes than to steric hindrance when 3 essential imino/amino functions, located close to the entrance of the catalytic cavity (His 40 and 57 residues and Ala 149 end chain residue), are oriented towards the negatively charged mineral surface. When these functions loose their positive charge, the orientation of the adsorbed enzyme is changed and a similar activity as in solution at equivalent pH is recovered. This result has a fundamental interest in all fields of research where enzymatic activity is monitored using reversible adsorption procedures.

Key words : α-Chymotrypsin ; protein adsorption ; enzymatic activity ; montmorillonite ; Fourier Transform-Infrared Spectroscopy.

Journal of Colloid and Interface Science 214 (1999) 319-332.
DOI : 10.1006/jcis.1999.6189

INTRODUCTION

Soil bacteria and fungi involved in the biodegradation of organic matter secrete extracellular enzymes (1, 2). These enzymes hydrolyze insoluble or adsorbed polymers, making soluble monomers able to reach microorganisms or roots, to be taken up across cell membranes by specific transport systems and then be metabolized (3). The effect of this extracellular enzyme activity is clearly expressed in the few min around the roots in soil, the rhizosphere (4). In particular, the positive effect of the symbiosis between fungi and plant roots, the mycorrhizal association, on the phosphorus and nitrogen nutrition of the host plant is in a large part due to the secretion of phosphatases (5-7) and proteases (8).

Soils have a large solid surface area and adsorptive capacities, mainly due to high surface energy of the clay fraction (9). Enzymes have a high affinity for the clays and their interaction with such surfaces leads to a decrease of both mobility and catalytic activity (10-18). Two interpretations are currently invoked to explain the experimentally observed pH shift of the optimal enzyme activity when adsorbed on electronegative surfaces such as clays: (i) a surface pH effect due to the presence of the enzyme active site in the double diffuse layer (19-23) and (ii) a pH-dependent modification of the adsorbed enzyme (13, 16, 24-29). We will here present experimental results in favor of a third mechanism, a pH-dependent orientation of the enzyme on the surface.

Our aim is to determine for α-chymotrypsin, taken as a model proteolytic enzyme of the rhizosphere, which interpretation of the interaction is most appropriate, and if structural and solvation changes induced by adsorption could be related to the changes of the enzyme activity.

Journal of Colloid and Interface Science 214 (1999) 319-332.
DOI : 10.1006/jcis.1999.6189

The pH dependence of the activity of this enzyme is modified by adsorption on a montmorillonite, clay with an electronegative surface (9). Using FTIR-transmission spectroscopy, we have quantified pD dependent structural secondary structures for α-chymotrypsin in solution and α-chymotrypsin adsorbed on the clay. The time resolved vibrational analyses allow specific ionization states of the acido-basic side chains to be related to local folding, or hydration, which appear to be determinant parameters for an optimum enzyme activity. Special attention is devoted to the various possible orientations of the adsorbed enzyme depending on the location of positively charged sites in the tertiary structure of the protein. The pD dependence was analyzed to determine which of these side chains could be involved in the adsorption process. The effect of a steric hindrance due to the clay will be discussed in relation to the pD dependent profiles measured for the enzymatic activity in solution and for the adsorbed protein.

MATERIALS AND METHODS

Chemicals

Dideuterium oxide (D_2O) were obtained from the CEA (France), NaD_2PO_4 and Na_2DPO_4 salts for the buffer by exchange in D_2O. A Wyoming montmorillonite with a size fraction < 2 μm, a specific surface area of 800 m^2/g, and an electric charge of 1.25 10^{-6} mol. e^-/m^2 was used. The α-chymotrypsin was purchased from Sigma [C 4129, type II, from bovine pancreas]. The crystalline protein has a 5×6×6 nm^3 size (30). It is made of 3 polypeptide chains linked by 5 disulfide bridges. Among the 241 amino-acid residues, 14 have carboxylic functions (9 Asp

Journal of Colloid and Interface Science 214 (1999) 319-332.
DOI : 10.1006/jcis.1999.6189

+ 5 Glu), 16, amino/imino (13 Lys + 3 Arg), 4, phenolic (4 Tyr) and 2 imidazole (2 His) functions. The isoelectric point (i.e.p.) is 8.6. In the crystalline state the secondary structure is made of parallel and antiparallel β−sheets for ~ 51% of the polypeptide backbone. Only 11% of the backbone have a helical structure (30, 31).

The substrate used for the measurement of the catalytic activity was the N-benzoyl-L tyrosine p-nitroanilide (BTNA) obtained from Sigma (B 6760). The reaction was stopped by addition of 1 mol/L trichloracetic acid, and the reaction product, aniline, was measured by its absorbance at 410 nm after two centrifugations of 10 and 15 min at 40 000 g. Citrate (pH<7), phosphate (7<pH<8) and borate (pH>8) buffers were used. The ionic strength of the buffers was estimated from the sodium ion concentration. The final concentrations used were 30 mg/L of α-chymotrypsin, 77 μM of BTNA, 0.7 g/L of montmorillonite, an ionic strength of 10 mM and the temperature was 25°C. The catalytic activity was measured *vs* pH following three procedures previously described (6, 13): (i) the chymotrypsin in solution, as a control, (ii) the chymotrypsin in presence of montmorillonite after 1 h of contact, containing both free and adsorbed chymotrypsin and (iii) in the supernatant after centrifugation (15 min at 40 000 g) of the chymotrypsin-montmorillonite suspension, measuring only the free fraction of the chymotrypsin.

FTIR spectroscopy

For protein in H_2O the contribution of the δOH of water directly bonded to the protein could be significant in the Amide I range. Moreover, this hydration can be modified

Journal of Colloid and Interface Science 214 (1999) 319-332.
DOI : 10.1006/jcis.1999.6189

by adsorption (32, 33). Thus for adsorbed hydrophilic proteins a quantitative analysis of Amide I absorption profiles exclusively in term of backbone structure and solvation is ambiguous. D_2O was used instead of H_2O (the δOD mode is in the 1200-1250 range). This raises the question of possible specific secondary structures in D_2O (34). Indeed, D_2O could reduce kinetics, but to date, CD (35), as NMR analyses performed on small proteins, have not displayed structural difference (36).

D_2O buffers (0.055 mol/L) were initially prepared at pD 8 with Na_2DPO_4 salts (pD = pH + 0.4) (37). DCl, or NaOD concentrated solutions in D_2O were added to the initial buffer (pD 8) to obtain 6 different pD in the 4-12.5 range. For the solutions, α-chymotrypsin was dissolved at 5 mg/mL (2.10^{-4} mol./L). The suspensions contained 5 mg/mL of chymotrypsin and 10 mg/mL of montmorillonite. All samples were prepared at room temperature (20-22°C) and in an Argon saturated glove-bag in order to avoid any H_2O contamination. The addition of α-chymotrypsin, or α-chymotrypsin-clay mixtures could modify the pD of the aqueous buffers adjusted with DCl or NaOD. The pD were always stabilized 2 hours after these additions. Especially for initial pD between 9.5 and 11.5, a slow decrease to *ca* 8.5 was always measured after adding α-chymotrypsin, or α-chymotrypsin and clay. In this pD range to reach a structural equilibrium, α-chymotrypsin apparently releases more protons than it captures. The difference, less than 10^{-8} mol/L proton, means that the ratio of slowly deprotonating acidic functions (COOH, Φ-OH) on slowly protonating amino/imino basic sites is greater than one. When using same initial buffers the resulting pD varied by less than 0.2 units. The averaged pD listed in Tables 1 and 2 result from sets of 2, 3, or even 4, reproducible

Journal of Colloid and Interface Science 214 (1999) 319-332.
DOI : 10.1006/jcis.1999.6189

experiments. These pD slightly differ from solutions to suspensions. Thus, comparisons between solution and adsorbed states had to be performed for pD that could differ by 0.2 unit. For 4<pD<9, the FTIR spectra of the supernatant for the α-chymotrypsin-clay suspensions, showed that more than 95% of the protein was adsorbed on the clay. For pD 11.8, half of the protein remained in the supernatant.

FTIR-transmission spectra were recorded on a Perkin Elmer 1720 spectrometer equipped with a DTGS detector. Resolution was set at 4 cm^{-1}, using boxcar. A Balston air dryer from Whatman (UK) strongly reduced the water vapor in the spectrometer during the measurements. Solutions were inserted into a CaF_2 cell with a 50 μm spacer. Suspensions of the solid phases were inserted between two CaF_2 plates with a 25 μm spacer allowing an easy cleaning. For each sample numerous spectra were collected from five minutes to three hours. Time zero was setup when the buffer was added onto the solid protein, or the solid protein-clay mixtures. Inside the spectrometer, after 10 minutes, the temperature was stable and the air dryer reached its maximum of efficiency.

Spectral differences were computed in the 1800-1350 cm^{-1} wavenumber range, on one hand between protein in solutions and the corresponding buffers and on the other hand between protein-clay mixtures and corresponding clay suspensions. Adjustments were made using a computed spectrum of HOD (difference spectrum between pure D_2O and partially hydrogenated D_2O spectra) so as to reduce as much as possible the HOD contribution in the 1470 cm^{-1} spectral range. The narrow and residual H_2O vapor bands were canceled by a slight spectral smoothing before second derivative treatments. Second derivative and curvature calculations were

performed on the difference absorption spectra, and compared to self-deconvolution procedures in order to establish for all spectra a same number of principal components in the 1800-1500 cm^{-1} range (38). The curvature analysis corresponds to a home made computed analysis, based on a second derivative, to amplify curvatures in a spectral profile and also to reduce the intensity of the lateral wings for the detected bands. Indeed the three methods gave for all spectra a similar number of principal components at similar wavenumbers (± 1 cm^{-1}, or less). Some of the initial difference spectra and also some second derivative or curvature spectra are reproduced in Figure 1. The slight wavenumber shifts of the identified components were not sufficient to be valuably introduced in our spectral fitting (34). Thus the same set of 9 Amide I (Tables 1, 2) and of 2 Amide II components (1549 and 1532 cm^{-1}) were introduced to compute the decomposition of all spectra. To fit the overall 1800-1500 cm^{-1} range, other bands were included (Fig. 2). They correspond to identified side chains (39, 40). Asp and Glu side chains give absorption *ca* 1715 cm^{-1} for νCO_{COOH}, 1584 (Asp) and 1567 cm^{-1} (Glu) for $\nu_a COO^{-1}$ modes 1605 and 1518 cm^{-1} are assigned to Tyr and 1592 cm^{-1} to Trp/His vibrations. The $COND_2$ functions of the Asn and Gln side chains (23 residues) should have significant contributions in the Amide I range (40). However, the corresponding frequencies are not predictable enough to valuably include specific Asn and Gln contributions in our curve fitting procedure. The same last square iterative program (Levenberg-Marquardt), with fixed empirical half band width at half band high (10 cm^{-1}) and also fixed empirical Lorentzian/Gaussian profile (0.25/0.75), has been applied (32, 33, 38, 41) to fit all difference spectra. These constant band shape parameters were empirically chosen to fit, for the best, all the spectra. Intensities were only allowed variations (Fig. 2). With so many constraints, although the number of components was important, computed intensities resulting from

Journal of Colloid and Interface Science 214 (1999) 319-332.
DOI : 10.1006/jcis.1999.6189

successive fits for one spectrum were always identical. We have also tested that decomposition of smoothed or unsmoothed spectra gave practically the same results with only 0.4 % variation for components with closest wavenumbers (1644 and 1638 cm^{-1}) and even less for the others. The constancy in frequencies and bands shapes for any spectral decomposition allows a comparative quantitative analysis of intensity changes for each component, from one spectrum to another.

Protein flexibility is related to the rate of the peptide NH/ND exchange in D_2O. This exchange is evaluated by the measurement of the decrease of Amide II intensities (residual CONH entities) as a function of time and expressed in % of the overall Amide I intensity (32, 33, 41). For totally hydrogenated α-chymotrypsin (solid state) Amide II/Amide I (area) reaches ~ 40 % (spectrum not shown). In solution, most of the random peripheral polypeptide segments are exchanged within 10 min. Then, the exchange depends on the diffusion of D_2O into internal domains. In all cases, 2 hours after α-chymotrypsin dissolution, the NH/ND exchange concerned more than ~65 % of the polypeptide backbone. The Amide II/Amide I intensities (%) plotted in Figure 3 are averaged values from two or more experiments prepared with the same buffer (cf. above). With careful control of time, temperature and spectrometer drying, there was less than 2 % variation between equivalent samples. As α-chymotrypsin consists of 241 residues, a decrease of the Amide II/Amide I ratio of 2 % should involve NH/ND exchange for ~ 12 peptide units.

Structural and solvation parameters evaluated for the protein backbone rely on the decomposition of the 1700-1610 cm^{-1} spectral range which mostly correspond to the vibrational motions of the CO peptide groups (Amide I for CONH, Amide I' for COND) (42-45). Indeed, in our study COND species always dominated the CONH. No major frequency shifts being observed as a function of time (cf. above), no distinction was made for Amide I for CONH or COND

Journal of Colloid and Interface Science 214 (1999) 319-332.
DOI : 10.1006/jcis.1999.6189

entities. Moreover, our analyses result from comparisons between α-chymotrypsin samples having a similar extent of exchange. Each Amide I component is expressed as the % of the overall Amide I intensity. The assignments of these Amide I components are given in Table 1 (32, 33, 39, 41-47). The two weak bands in the 1690-1680 cm^{-1} spectral range are associated to peptide CO in hydrophobic environments (32, 33, 41). α-Chymotrypsin contains a large amount of β-sheets, thus a small contribution of these structures is also expected in this spectral range (see further) (34, 39, 44). The two next components *ca* 1670 cm^{-1} and 1660 cm^{-1} are assigned to not hydrogen bonded peptide units in loops in polar environments (46, 47). The 1651-cm^{-1} component is assigned to the helical domains. The estimated amount of CO peptide groups involved in helical structure, *ca* 15 %, is in agreement with the weak proportion of amino acid residues involved such structure (12 %) determined by X-ray spectroscopy for α-chymotrypsin (30, 31). The major band at 1638 cm^{-1} and another at 1630 cm^{-1} are associated with β-sheets. Adding both contributions, for example 25 and 16 % for respectively for α-chymotrypsin at pD 5.6, the proportion of CO peptide groups H-bonded in β-sheets reaches 41%. This is also in good agreement with X-ray spectroscopy for crystallized chymotrypsin giving 52 % amino acid residues involved into double or triple strand β-sheets (30, 31). Indeed, in double strand β-sheets, only half of the CO peptide units are H-bonded. The relatively wide frequency range accounting for β-structures could arise from the presence of both parallel and anti parallel extended strands (30, 31, 44). An alternative assignment is proposed by Casal and *al.* (48): the 1630 cm^{-1} component could correspond to external β-sheets exposed to solvent, then hydrated. At *ca* 1618 cm^{-1} a weak component is assigned to external polypeptide extended strands that could be self-associated to other external strands of adjacent protein molecules (42, 48-51). Accounting for

Journal of Colloid and Interface Science 214 (1999) 319-332.
DOI : 10.1006/jcis.1999.6189

correlation between increased adsorption in the 1645-1635 cm^{-1} spectral range and increased rate of the NH/ND exchange for several proteins (32, 33, 39, 41), we propose to ascribe the increase of the 1644 cm^{-1} component for α-chymotrypsin to an increase of backbone hydration in random domains.

Intensities (%) reported in Tables 1 and 2, and plotted in Figures 3, 9, 10, correspond to averages (*cf.* above). Before averaging, variations in intensity of the Amide I components for equivalent samples were less than 1 %. Weak variations of the Amide I molecular extinction coefficient from on peptide species to another are expected. Thus, the calculated percentages cannot precisely indicate the absolute amounts of each species. However, any difference, ± 1 %, or more, measured as function of time, or from one pD to another, or from a solution to an adsorbed state, is assumed to be significant of solvation and/or structural changes. As α-chymotrypsin consists in 241 residues, such change of 1 % should involve 2 or 3 peptide units.

RESULTS AND DISCUSSION

α-Chymotrypsin in solution

NH/ND Exchange 10 min to 2h

The time dependent evolution of the Amide II/Amide I intensities (%), relative to the amount of residual CONH units, are plotted in Figure 3 A, for 6 pD. At any given time, this ratio

Journal of Colloid and Interface Science 214 (1999) 319-332.
DOI : 10.1006/jcis.1999.6189

decreases for increasing pD. We conclude that the increase of the pD enlarges the flexibility of the chymotrypsin backbone.

The increase in exchange from pD 4.5 to pD 5.5, at 10 min, arises from the deprotonation of the 3 carboxylic end chains and the external Asp and Glu carboxylic groups (pK 3.3-4.3) displayed in the schematic representation of crystallized Alpha-chymotrypsin (tosylated), PDB 2CHA : from J. J. Birktoft and D. M. Blow-1975 (31). The decrease in absorbance in the 1700-1750 cm^{-1} range (Fig. 1) and the increase of the $\nu_s COO^-$ bands, *ca* 1584 and 1567 cm^{-1} (not shown), illustrate this deprotonation. The slope of the curve from 10 min to 45 min (Fig. 3 A) is steeper at pD 5.5 than at pD 4.5. During this period, the residual νCO_{COOD} absorption decreases (not shown). This implies that the few carboxylic functions still protonated at pD 4.5 are slowly deprotonted at pD 5.5. They should correspond to the buried Asp-102 and -194 and Glu -70 side chains (Fig. 4). New internal hydrophilic sites (COO^-) would favor the diffusion of more water molecules into protein cavities.

For pD 7.5 the exchange before 10 min is strongly enhanced, thereafter the curve is parallel to that for pD 5.5. (Fig. 3 A). At pD 7.5 all carboxylic functions are deprotonated at 10 min as indicated by the absence of any residual absorption in the 1740-1700 cm^{-1} range. The 2 His imidazole side chains (40 and 57), protonated at pD 5.5, should remain unprotonated in aqueous medium at pD 7.5 (pK ~ 6). Salt bridges between His^+ and the internal carboxylates side chains (Asp-194, Asp-102, Glu-70) that could be formed between pD 5.5 and 6.5 (Fig. 5), should be disrupted when His side chains become neutral. This apparently enhances the amount of water inside the enzyme core, allowing the exchange of ~30 more peptide units.

Journal of Colloid and Interface Science 214 (1999) 319-332.
DOI : 10.1006/jcis.1999.6189

At pD 8.6, in agreement with the deprotonation of all carboxylic groups and imidazole side chains, as for pD 7.5, the NH/ND exchange at 10 min is not increased further. However, from 20 min up to 2 h a significant enhancement of the exchange is observed once more. At pD 7.5 the three amino end terminal groups (Cys-1, Ile-16, Ala-149) should be protonated (pK ~8.3) (Fig. 6). At pD 8.6 they should be mostly unprotonated. Indeed, in the crystalline state, Asp-194 is close to the Ile-16 amino end chain (Fig. 5). The slow increase of the exchange could depend on a specific enlarged water solvation if a salt bridge between Asp-194 carboxylate and aminium Ile-16 chain cannot be formed (52). The uncompensated negative charge inside the enzymatic cavity would entail greater water diffusion exchanging about 20 more peptide units.

Similarly an increase of the pD to 11.6 does not have much effect on the NH/ND exchange at 10 min. This agrees with the external position of all Lys (pK 10.5) which should stay deprotonated, rather than protonated at lower pD, without modifying the internal hydration (Fig 6). A fast deprotonation of the 2 external Tyr side chains (Fig. 7) should also occurred (pK 10.1). From 20 min up to 2 h the exchange becomes greater than at pD 8.6. This is associated to the slow deprotonation of the 2 internal Tyr residues (Fig. 7).

At pD 12.4, a weak supplementary exchange is detectable from the first measurements. A partial deprotonation of the relatively external imino Arg-154 chain (pK 12.5) could weaken a bridge with the adjacent Asp-72 carboxylate function and separates two close and relatively hydrophobic peptide strands (Fig 8). Such a structural transition would have favored an immediate exchange of the adjacent peptide domains.

Secondary Structures and Hydration

Journal of Colloid and Interface Science 214 (1999) 319-332.
DOI : 10.1006/jcis.1999.6189

The spectral decompositions were performed for spectra recorded at 10, 20, 30, 45, 60 and 120 min, at 6 pD. The evolution of the intensity of 4 Amide I components (%) representative of β-sheet secondary structures, direct backbone hydration and protein self-association, as a function of time, are only illustrated for pD 4.5 and 11.6, in Figure 9 A and B, respectively.

For pD 4.5 the intensity of all Amide I components remains practically constant between 10 min and 2 h (less than 1 % variation) meaning that the structural equilibrium, with external carboxylate and internal carboxylic side chains (Fig. 4) was established within 10 min. For pD 5.5 some variations with time were noted (not shown). While the relatively peripheral His residues are assumed to be rapidly protonated, a slow deprotonation of the internal carboxylic functions should occur, as inferred from the study of the NH/ND exchange (Fig. 3 A).

For pD 7.5, because equilibrium was attained within 30 min (not shown), internal Asp and Glu side chains were assumed to be rapidly deprotonated and His imidazole groups to remain unprotonated. For pD 8.6, between 10 min and 1 hour, a slight decrease of β-structure (1638 cm^{-1}) was compensated by direct hydration of ~3-4 peptide units (1644 cm^{-1}, not shown). This could reflect slow structural changes at Asp-194 and Ile-16 levels (Fig. 5).

For pD 11.6, some unstability was also observed from 10 min to 1 h (Fig. 9 B). A small amount of β-structure (1638 cm^{-1}) is transformed into another kind of β-folding (1630 cm^{-1}) and also into directly hydrated peptide units (1644 cm^{-1}). The overall slow structural variation concerns 5-7 peptide units. In agreement with the NH/ND exchange results (Fig. 3 A), this could be related to slow deprotonation of the internal Tyr residues (Fig. 7). As before, there was no more than 1 %

Journal of Colloid and Interface Science 214 (1999) 319-332.
DOI : 10.1006/jcis.1999.6189

variation between 1 and 2 h. Thus, at any studied pD, α-chymotrypsin in solution was assumed to reach a structural and solvation equilibrium after 2 hours.

Only the intensities of the Amide I components obtained after 2 hours are displayed in Table 1. They are plotted as function of pD in Figure 10. The evolution of the secondary structures are shown in part A. The evolution of the solvation state of the peptide backbone, with ″free″ (polar and hydrophobic), or hydrogen bonded carbonyls are shown in part B. The H-bonded carbonyls are either bonded with water molecules, or with peptide -NH- from adjacent protein molecules (protein self-association). The intensities of the Amide I components assigned to ″free″ internal carbonyls are almost pD independent. These domains are not influenced by the ionization states of the acido-basic side chains of the protein. The very weak decrease of the α-helix content when pD increases means that the two external helical regions in chymotrypsin are not strongly affected by electronic charges carried by the acido-basic side chains (Fig. 4, 6).

From pD 4.5 to pD 5.6 and 7.5, the slight decrease of the component at 1644 cm^{-1}, means a weak reduction of the direct peptide hydration. In the mean time, both Amide I components for β-structures, at 1638 and 1630 cm^{-1}, increase simultaneously (Table 1, Fig. 10 A). Such changes concerns 8-12 peptide units in all. The local folding is apparently all set when the deprotonation of internal carboxylic side chains is completed. An internal electrostatic interaction between the COO^- group of Asp-194 and the NH_3^+ group of Ile-16 could have favored this constraint (Fig.5). The larger NH/ND exchange measured from 4.5 to pD 5.5, then to 7.5 (Fig. 3 A) contrasts with this result. The deprotonation of the overall carboxylic functions (17 functions, including the 3 end chains) (Fig. 4), all becoming highly hydrophilic, could have as for the NH/ND exchange rate, overcame the effect of the local folding depending on an Asp-194···Ile-16 salt bridge.

Journal of Colloid and Interface Science 214 (1999) 319-332.
DOI : 10.1006/jcis.1999.6189

On the contrary, at pD 8.6, the increase of the component at 1644 cm^{-1} demonstrates an increase of direct hydration (Table 1 and Fig. 10 B). This is connected with a decrease in β-sheet (1638 cm^{-1} in Table 1). Indeed, the other kind of β-structure (1630 cm^{-1}) slightly increases (Table 1). The changes only concern 8-12 peptide units in all (Fig. 10 A, B). Thus, a parallel strand becoming antiparallel is unlikely. The assignment of the 1630-cm^{-1} band to new hydrated β-domains (48) is in better agreement with the simultaneous direct backbone hydration (Fig. 10 A) and the faster NH/ND exchange (Fig 3 A). At pD 8.6, in comparison to pD 7.5, the disruption of the salt bridge between Ile-16 and Asp-194 (Fig. 5) could have entailed these structural and solvation changes.

From pD 8.6 to 11.6 the contribution of β-structures decreases strongly (52) and hydration increases in random and β-domains (Table 1 and Fig. 10 A, B). At pD 11.6, the two His imidazole, the 3 amine end chains and all Lys side chains should stay unprotonated (Fig. 6). These changes and a fast deprotonation of the 2 external Tyr residues (171 and 146) (Fig 7) are assumed to involve structural changes in relatively peripheral regions. Then slow proton transfers involving the internal Tyr-228 (Fig. 7) and close internal Arg-230 residues could lead to the slower secondary transition between 10 min and 1 h (Fig. 9 B). This different charge distribution to that at pD 8.6, gives rise to new structural and solvation features (Fig. 10 A, B). In agreement with a previous Raman study (52) the β-sheet unfolding concerns 10-15 peptide units. It is followed by an increased hydration of *ca* 10 % of the backbone, meaning around 20-30 internal peptide units.

Compared to pD 11.6, only a very small β-domain is unfolded at pD 12.4 (~3 peptide units). Internal hydration remains practically constant, but some more protein self-association is

Journal of Colloid and Interface Science 214 (1999) 319-332.
DOI : 10.1006/jcis.1999.6189

observed. Self-association minimizes contacts between water and unfolded hydrophobic domains of the protein. This implies that the extra unfolding at pD 12.4 rather concerns an hydrophobic region. As proposed from the NH/ND exchange analysis, the partial Arg-154 unprotonation could disconnect two external neighboring strands in the protein (Fig. 8). A larger flexibility of these hydrophobic domains would favor protein self-association in solution. In the pD range 4.5-8.6, the 1618 cm^{-1} Amide I component is weak and constant, indicating that at the concentration used (5 mg/mL) protein aggregation is very weak, if any. Indeed, in this pD range the component at 1618 cm^{-1} could be assigned to a vibrational contribution of the Tyr-OH side chains (40). When these side chains are deprotonated ($Tyr\text{-}O^-$) the vibrational mode is lowered to 1604 cm^{-1} (53). Thus in the present case, the increase of the absorbance at 1618 cm^{-1} from pD 11.6 pD 12.4 when all Tyr side chains should be deprotonated, are not assigned to tyrosinate side chains, but to protein self-association.

Correlation between NH/ND Exchange, Structure, Solvation and Enzymatic Activity

The pH dependence of α-chymotrypsin catalytic activity is presented in Figure 11. Below pH 5 the enzyme has no activity. Our results for pD 4.5 (pH 4.1) emphasize on that such inactivity is not related to protein denaturation, but to the protonation state of the internal Asp and Glu side chains. Carboxylate forms are essential in the catalytic process (54-56).

From pH 5 to 7 (pD 5.4 to 7.4), the hydrolytic activity of α-chymotrypsin increases progressively. The NH/ND exchange, and thus water diffusion, was also increased. According to the pH dependence of the activity, only the fraction of protein with unprotonated imidazole is assumed to

Journal of Colloid and Interface Science 214 (1999) 319-332.
DOI : 10.1006/jcis.1999.6189

be active. When the maximum of the activity is reached, Ile-16 amino end chain is apparently still protonated. Its interaction with Asp-194 appears to draw a specific favorable folding. Indeed, when the structural contraction is released at pD 8.7 (pH 8.3) the catalytic activity decreases. The catalytic activity of α-chymotrypsin is known to depend on pH dependent His^+ proton transfers (54-56). A local unfolding depending on the disruption of an Asp-194….Ile-16 salt bridge has also been suggested (57).

At pH above 10.5 the enzyme has no more activity. Our analysis in the 11.2 - 12 pH range (pD 11.6 - 12.4) confirms an unfolding of β-secondary structures (52). Most of the changes are assumed to be in relatively peripheral domains, but other more internal changes could be connected with the deprotonation of the 2 internal Tyr residues (Fig. 7). Too many water molecules inside the catalytic cavity could interfere with polar functional groups of the substrate (56). Indeed, a negative charge on Tyr-146 end chain, not far from the entrance of the catalytic cavity (Fig. 7), might have also cancelled the affinity of the enzyme for its substrate.

α-Chymotrypsin Adsorbed on Montmorillonite

NH/ND Exchange from 10 min to 2 h

The time dependence of the amount of residual CONH peptide units (Amide II/Amide I %) for α-chymotrypsin adsorbed on montmorillonite in presence of D_2O, are shown in Figure 3 B, for 5 pD.

Journal of Colloid and Interface Science 214 (1999) 319-332.
DOI : 10.1006/jcis.1999.6189

At pD 4.5, the exchange is reduced at 10 min compared to solution, while in contrast, it is favored from 30 min up to 2 h. Adsorption is assumed initially to prevent relatively peripheral domains of the protein from contact with water. However, the greater exchange later (2 h) proves that water molecules finally penetrate further inside the protein.

For pD 5.9, in comparison to pD 4.5, the NH/ND exchange initially increases (10 min). Then the time dependent profiles are parallel. Initially adsorption reduced the exchange with respect to solution (pD 5.5), then the exchange is enhanced. In first stage, adsorption protects weakly buried domains, but after 1 h, internal domains finally encounter more water molecules than in solution. For the solutions, the enhanced exchange from pD 4.5 to 5.5 was associated with the deprotonation of the internal carboxylic side chains (Fig. 4). For the adsorbed state, the intensity of the νCO absorption of the carboxylic groups (1700-1750 cm^{-1}) as a function of pD, followed that in solution (Figs. 1 and 2). Based on this observation, the time dependence of the NH/ND exchange should have been similar for the two states.

Once again, at pD 7.7 adsorption prevents some NH from the exchange for the first hour. However, in contrast to lower pD, after 2 h, the exchange is similar for the adsorbed and solution states. Such similar exchange for the buried peptide units emphasizes that specific features induced by adsorption do not involve buried domains of the protein.

At pD 8.7, at 10 min, the exchange for the adsorbed protein exceeds that for the protein in solution meaning that the clay no longer protects external domains of the protein from water contact. The similar exchange measured after 2 h, when water reaches internal domains confirms that, as at pD 7.7, adsorption involved only external domains of the protein.

Journal of Colloid and Interface Science 214 (1999) 319-332.
DOI : 10.1006/jcis.1999.6189

For pD 11.8, the NH/ND exchange was also initially faster in presence of montmorillonite, but to a lesser extent than at pD 8.7. The difference concealed rapidly (30 min). Compared to the solution (pD 11.6), at 2 h adsorption even seems to prevent exchange in buried or hydrophobic regions. Indeed, for this pD we have found half of the protein in the supernatant (*cf*. experimental). We assume that protein molecules exchanging on the electronegative surface are, in average, structurally influenced by this surface.

Secondary Structures and Hydration (2 h)

For α-chymotrypsin adsorbed on montmorillonite, decompositions were also performed for spectra recorded 10, 20, 30, 45, 60 and 120 min, at 5 pD. The time dependencies of the Amide I components for pD 4.5 and 11.8 are plotted in Figure 9, C and D, respectively, as examples.

At pD 4.5 (Fig. 9 C) and 5.9 (not shown), the time required to attain structural equilibrium is longer than for the solutions (Fig. 9 A). Several external protonated Lys and Arg side chains, the two peripheral His^+ side chains and the flexible Ala-149 aminium end chain, which are oriented on the same side of the protein should be rapidly adsorbed by the electronegative clay (Figs. 6 and 12). From 10 to 40 min, given the slower NH/ND exchange for the adsorbed state (Fig. 3 B), the amount of water which reaches internal hydrophilic domains of the protein is reduced by the steric hindrance of the clay. Then, for the adsorbed state, a slow conformational modification of the protein, from 30 min to 1 h, finally favors hydration in internal random and β-domains (Fig. 9 C) corroborated with the larger NH/ND exchange (from 40 min to 2 h, Fig. 3 B). Adsorption also entails some protein self-association.

Journal of Colloid and Interface Science 214 (1999) 319-332.
DOI : 10.1006/jcis.1999.6189

For pD 7.7, as for the solution, the conformation of the adsorbed protein was stabilized at *ca* 30 min (not shown). At this pD the His imidazole groups should remain unprotonated but the external Ala-149 and internal Ile-16 amino end chains protonated (Fig. 6). At pD 8.7, some fluctuations are noted between 30 and 40 min (not shown). As for the solution in this pD range, these fluctuations are related to proton exchange at the internal Ile-16 aminium/amine end chain.

For pD 11.8, the slow enhancement of the hydration in β-structures and in random domains from 10 to 30 min (Fig. 9 D) is related to a slow deprotonation of the 2 internal Tyrosine side chains, as in solution (Fig. 7). In comparison to solution (Fig. 9 B), the reduction of the slow internal hydration (from 40 min to 2 h) confirms an influence of the clay on chymotrypsin, even in this pD range (Fig. 9 D).

The Amide I intensities given in Table 2 and plotted in Figure 10 C and D, provide information on the structure and solvation of chymotrypsin adsorbed on montmorillonite at various pD, when structural equilibrium has been reached (2 h). An increase of the pD from 4.5 to 11.8 obviously induces less change for the adsorbed protein than for the protein in solution (Fig. 10). This is good agreement with the weaker pD dependence of the NH/ND exchange after 2 h (Fig. 3). As for the exchanges, the larger effects of the clay on chymotrypsin are detected at pD below 7.7 (Tables 1, 2 and Fig. 10).

At pD 4.5, helical domains (Fig. 8) are only very slightly reduced (Fig. 10 C) compared to the solution (Fig. 10 A). The larger unfolding concerns β-sheets ~10-15 peptide units. Hydrated β-sheets (1630 cm^{-1}) become dominant over the not hydrated ones (1638 cm^{-1}) and direct hydration is also enhanced (1644 cm^{-1}) (Tables 1 and 2 and Fig. 10). These changes apparently take place in two steps : a first state is reached within 10 min and a second step lasts to 1 h. The new features

Journal of Colloid and Interface Science 214 (1999) 319-332.
DOI : 10.1006/jcis.1999.6189

cannot arise from a different $COOD/COO^-$ ratio for Asp or Glu side chains in the adsorbed state (*cf.* above). The primary changes are associated with a rapid orientation of positively charged external functions towards the electronegative surface (Figs 6 and 12). An optimization of these interactions with the mineral surface over 40 min would explained the slower secondary structural transition. This is in complete agreement with the progressive unshielding of some peptide units, which are easily exchanged once all the structural transitions induced by adsorption are established.

For pD 5.9 the unfolding resulting from adsorption is larger than at pD 4.5 (~ 20-25 peptide groups) (Fig. 10 A, C). For the solutions, increasing pD from 4.5 to 5.6 entailed specific dehydration and weak β-folding (Table 1, Fig. 10 A, B). This folding is apparently restricted by adsorption (Table 2, Fig. 10 C, D). The orientation of the His^+ side chains and Ala-149 aminium end chain towards the clay surface could hinder cooperative internal electrostatic interactions between imidazoles, carboxylates and aminium end groups (Fig. 5) favoring the β-folding observed in solution.

At pD 7.7, although water diffusion inside the protein at 2 h is similar to what happens in solution (Fig. 3), the level of secondary structure remains weaker (Tables 1, 2 and Fig. 10 C). This confirms that most of the unfolding concerns relatively peripheral regions (~ 10-15 peptide units). On the other hand, the local folding observed in solution at pD 5.9 and 7.5 (Fig 10 A) is now set up for the adsorbed state (Fig. 10 C). When His imidazole groups are unprotonated (uncharged) they are no longer oriented towards the clay surface. The orientation of the adsorbed protein could have enabling the imidazole side chains to adopt structural arrangements allowing the formation of the Asp-194···Ile-16 electrostatic bond as in solution (Fig. 5).

Journal of Colloid and Interface Science 214 (1999) 319-332.
DOI : 10.1006/jcis.1999.6189

At pD 8.7, the level of unhydrated β-sheet remains lower for the adsorbed state (Tables 1, 2), but as in solution, the local β-unfolding is observed. Thus, direct hydration becomes similar in the solution and adsorbed states (Tables 1, 2, Fig. 10 B and D). These features occur just when the NH/ND exchange profiles are the closest for the two states (Fig. 3). In both cases, the deprotonation of the Ile-16 end aminium chain should entail the same Asp-194$^{\cdots}$Ile-16 salt bridge disruption.

For pD 11.8, the small differences between solution and the adsorbed state arise from slight reductions of direct hydration and hydrated β-structures (Tables 1, 2, Fig. 10). This confirms that besides a greatly reduced number of positive charges around the globular protein and in spite of its global negative charge, chymotrypsin is still influenced by the electronegative clay. This could be via the external Arg^{+}-230 residue located on the opposite side of many Lys side chains (Fig 12). Compared to pD 8.6, at pD 11.8, the protein with numerous deprotonated Lys side chains should adopt another orientation on the clay. Specific interactions via Arg^{+} side chains could specifically shield an internal domain reducing its direct hydration on one hand and the rate of the exchange in nearby domains on the other hand (see above).

All along the 4.5-11.8 pD range adsorption entails some protein self-association (Fig. 10 D). Self-association should involve relatively peripheral unfolded hydrophobic domains (33, 41).

Correlation between NH/ND Exchange, Structure, Solvation and Enzymatic Activity

Adsorption completely inhibits enzyme activity below pH 7. The catalytic activity is reduced between pH 7 and 8.5, but recovers above pH 9 (Fig. 11). Indeed a major result of our analysis is

Journal of Colloid and Interface Science 214 (1999) 319-332.
DOI : 10.1006/jcis.1999.6189

that the unfolding induced by adsorption are weak and concerns essentially peripheral domains of the protein (10-15 peptide units). This should not perturb the structure at the level of the enzymatic site.

Thus, the mechanism responsible for the decrease of enzyme activity on adsorption is probably not a pH dependant modification of conformation as previously described for several proteins: bovine serum albumin (26); Hebeloma cylindrosporum acid phosphatases (6); sweet almond (13) and Apergillus niger (16) β-D-glucosidases. In this model, it is assumed that the protein unfolds below its isoelectric point, due to strong attractive electrostatic forces between the positively charged protein and the negatively charged clay surface.

Since adsorption has practically no effect on the enzyme activity above pH 9, unfolding associated with Lys^+ adsorption cannot be responsible for the inhibition observed at lower pD. Electrostatic interactions between these side chains and the clay should not hinder the access of the substrate into the enzymatic site (Fig 13). For pH lower than 6.5 (pD ~ 7), the presence of the clay close to the two His^+ imidazole groups and to the Ala-149 aminium end chain, located at the entrance of the enzymatic cavity, could be the reason for complete protein inactivation (Fig. 12). However, just above pH 7, when most of His side chains should be deprotonated, the enzymatic activity is far from entirely recovered. In this pH range, proton exchange at the imidazole sites, favorable for enzyme activity, could maintain the adsorbed protein with an orientation still shielding the catalytic site. Indeed protein orientation changes should be very slow compared to proton transfers on the nitrogenous imidazole. Moreover, in this pD range the protonated Ala-149 aminium end chain, at the entrance of the catalytic cavity, could still interact with the mineral surface (Figs 5, 12 A). For increasing pH (pD 7.7), the orientation of the protonated Ile^+-16 end

Journal of Colloid and Interface Science 214 (1999) 319-332.
DOI : 10.1006/jcis.1999.6189

group towards Asp-194 could result from a change of the protein orientation, as expected with a partially deprotonated Ala-149 amino function. This allows some recovery of enzyme activity. In solution activity is effectively optimum when the salt bridge Asp-194···Ile-16 is set up. For the adsorbed state, the complete deprotonation of the Ala-149 amino group which only expected at pD 9, appears to be a prerequisite for complete release of the entrance of the enzymatic cavity from the mineral surface.

Such a mechanism, where decrease of catalytic activity is linked to an orientation of the active site towards the surface, has been already described on a ribonuclease A adsorbed on mica (58). Ribonuclease A is a "hard" protein (59, 60) which has a relatively large dipole moment of its charge distribution with the positive end pointing towards the region of the active site (61). With time, a translation diffusion process leads to molecular reorientation of ribonuclease. A side-on adsorption with the active site facing the mica surface in initial stages is followed by a progressive "standing-up" of the enzyme which exposes the active site to the solution, hence an access for the substrate.

CONCLUSIONS

In contrast to complete 3-dimensional structure of proteins that can be established using NMR spectroscopy, the approach by FTIR spectroscopy is currently limited to an average description of protein secondary structures and backbone solvation states. However, with FTIR, much larger proteins can be studied and structural parameters obtained for a protein in solution can be compared to results obtained in an adsorbed state (32, 33, 41, 62-66). This has a

Journal of Colloid and Interface Science 214 (1999) 319-332.
DOI : 10.1006/jcis.1999.6189

fundamental importance since protein properties, in many cases, depend on their direct environment. When the 3-dimensional crystalline structure of the protein is known, it can be used as a reference state. FTIR analyses then become a high performance, fast and cheap experimental technique to evaluate of the amplitude of structural deformations resulting from local ionization changes, mutation (32) or from adsorption on electrostatic (62-64), or hydrophobic solid phases (32, 33, 41).

In the case of the well known the α-chymotrypsin proteolytic enzyme, the present transmission-FTIR analysis of solutions confirms that the optimum catalytic activity *ca* pH 8 results from the convergence of numerous parameters: (i) the deprotonation of the carboxylic side chains, (ii) the deprotonation of the 2 His side chains, increasing both protein flexibility and hydration, (iii) a local β-sheet folding resulting from the formation of a salt bridge between Ile^{+}-16 end chain aminium group and the Asp-194 side chain carboxylate. For pH > 10 the complete inhibition of the catalytic activity should result not only from peripheral secondary structure unfolding directed by external Lys or Tyr deprotonations, but also from internal Tyr deprotonations entailing excessive internal hydration in the vicinity of the catalytic center. For even higher pH, partial aggregation of the protein in solution is detected.

Our analysis also demonstrates that over the entire pD range investigated adsorption of α-chymotrypsin on montmorillonite is mainly determined by electrostatic interactions (6, 13, 16, 26, 27, 29). When the protein and the clay are brought into contact these interactions result in a dynamic structural transition of the protein which can last up to 1 h. In the 4.5-9 pD range the unfolding resulting from the adsorption involves about 15-20 peptide units in peripheral β-sheets. Protein flexibility and hydration are slightly enhanced with respect to solution phase. However,

Journal of Colloid and Interface Science 214 (1999) 319-332.
DOI : 10.1006/jcis.1999.6189

the pH dependent profile of the inactivation of the enzyme in the 5-9 pH range cannot be explained by these changes alone. Most of the inhibition would arise from a steric hindrance of the clay due to its interaction with positively charged His (40 and 57) imidazole and Ala^{+}-149 end chain aminium that control the initial specific recognition of the enzyme for its substrate. At pH higher than 8.5 when the charges at His and Ala-149 are completely released, the enzyme is adsorbed with a different orientation which allows a recovery of activity, similar to that measured in solution in the same pH range. This infers that neither peripheral unfolding, nor partial self-association of α-chymotrypsin cancels the enzyme activity. These findings have important implications for the immobilization of active proteases or enantioselective proteins on various supports (to be published). Furthermore they are of fundamental interest in research fields involving the pH dependence of reversible enzymatic activity. At pH > 11, the enzyme activity is completely inhibited both in the adsorbed state and in solution. We propose a dynamic and non-denaturing exchange between protein molecules in solution and those only weakly retained on the clay via isolated Arg^{+} side chains to account for their structural similarities. In relation to the stability of proteins at solid-liquid interfaces, these findings put the α-chymotrypsin in the class of the "hard" proteins, such as bovine pancreas ribonuclease (59, 60). In contrast the "soft" proteins, such as bovine serum albumin (26-29, 59, 60, 63) and some phytases (61) show larger conformational modifications on adsorption on solid surfaces.

ACKNOWLEDGMENTS

The authors thank Dr S. Staunton for critically reading the manuscript.

Journal of Colloid and Interface Science 214 (1999) 319-332.
DOI : 10.1006/jcis.1999.6189

REFERENCES

1. Burns, R. G., *in* "Soil Enzymes" (R. G. Burns, Ed.), pp. 295. Academic Press, New York, 1978.

2. Theng, B. K. G., *in* "Formation and Properties of Clay-Polymer Complexes" (B. K. G. Theng, Ed.), pp. 157. Elsevier, Amsterdam, 1979.

3. Burns, R. G., *Soil Biol. Biochem.* **14**, 423 (1982).

4. Tarafdar, J. C., and Jungk, A., *Biol. Fertil. Soils* **3**, 199 (1987).

5. Tarafdar, J.C., and Marschner, H., *Soil Biol. Biochem.* **26**, 387 (1994).

6. Leprince, F., and Quiquampoix, H., *Eur. J. Soil Sci.* **47,** 511 (1996).

7. Mousain, D., Matumoto-Pintro, P., and Quiquampoix, H., *Rev. For. Fr.* **49** (n° sp.) 67 (1997).

8. Plassard, C., Chalot, M., Botton, B., and Martin, F., *Rev. For. Fr.* **49** (n° sp.) 82 (1997).

9. Chassin, P., Jouany, C., and Quiquampoix, H., *Clay Miner.* **21,** 899 (1986).

10. McLaren, A. D., *J. Phys. Chem.* **58**, 129 (1954).

11. Armstrong, D. E., and Chesters, G., *Soil Sci.* **98**, 39 (1964).

12. Albert, J. T., and Harter, R. D., *Soil Sci.* **115**, 130 (1973).

13. Quiquampoix, H., *Biochimie* **69,** 753 (1987).

14. Quiquampoix, H., *Biochimie* **69,** 765 (1987).

15. Fusi, P., Ristori, G. G., Calamai, L. and Stotzky, G. *Soil Sci. Soc. Am. J.* **21**, 911 (1989).

16. Quiquampoix, H., Chassin, P., and Ratcliffe, R. G., *Prog. Colloid Polym. Sci.* **79,** 59 (1989).

17. Gianfreda, L., and Bollag, J. M., *Soil Sci. Soc. Am. J.* **58**, 1672 (1994).

18. Violante, A., De Cristofaro, A., Rao, M. A., and Gianfreda, L., *Clay Miner.* **30**, 325 (1995).

19. McLaren,A. D., and Estermann, E. F., *Arch. Biochem. Biophys.* **68**, 157 (1957).

20. Durand, G., *C. R. Acad. Sci.* **259**, 3397 (1964).

21. Goldstein, L., Levin, Y., and Katchalski,E., *Biochemistry* **3**, 1913 (1964).

22. Aliev, V. S., Gusev, V. S., and Zvyagintsev, D. G., *Vestn. Mosk Univ. Biol. Pochvovied.* **31**, 67 (1976).

23. Douzou, P., and Petsko, G. A., *Adv. Protein Chem.* **36**, 423, (1984).

24. Sandwick, R. K., and Schray, K. J., *J. Colloid Interface Sci.* **115**, 130 (1987).

25. Sandwick, R. K., and Schray, K. J., *J. Colloid Interface Sci.* **121**, 1 (1988).

26. Quiquampoix, H., and Ratcliffe, R. G., *J. Colloid Interface Sci.* **148,** 343 (1992).

27. Quiquampoix, H., Staunton, S., Baron, M. H., and Ratcliffe, R. G., *Colloids Surf. A: Physicochem. Eng. Aspects* **75,** 85 (1993).

28. Staunton, S., and Quiquampoix, H., *J. Colloid Interface Sci.* **166,** 89 (1994).

29. Quiquampoix, H., Abadie, J., Baron, M. H., Leprince, F., Matumoto-Pintro, P. T., Ratcliffe, R. G., and Staunton, S, *in* "Proteins at Interfaces II: Fundamentals and

Applications" (T. H. Horbett and J. L. Brash, Eds), ACS Symposium Series No 602, p. 321. American Chemical Society, Washington, 1995.

30. Mattews, B. W., Sigler, P. B., Henderson, R., and Blow, D.M., *Nature* **214**, 652 (1967).

31. Birktoft, J. J. and Blow, D. M., PDB, 2CHA (1975).

32. De Collongue, B., Sebille, B. and Baron, M. H., *Biospectros*. **2**, 101 (1996).

33. Boulkanz, L., Balcar, and Baron, M. H., *Applied Spectrosc*. **49**, 1737 (1995).

34. Caughley, B. W., Dong, A., Bhat, K. S., Ernst, D. S. F., and Caughey, W. S., *Biochemistry* **30**, 7672 (1991).

35. Dong, A., Matsuura, J., Allison, S. D., Chrismann, E., Manning, M. C., and Carpenter, J. F., *Biochemistry* **35**, 1450 (1996).

36. Nigles, M., and O'Donoghue, S. I., *Progr. Nucl. Magn. Reson. Spectr*. **32**, 107 (1998).

37. Glasoe, P. K., and Long, F. A., *J. Phys. Chem*. **64**, 188 (1960).

38. Baron, D., *in* "Logiciels pour la chimie", (Soc. Française de Chimie, Ed.), pp 282. Paris, 1991.

39. Wantyghem, J., Baron, M. H., Picquart M., and Lavialle, F., *Biochemistry* **29**, 6608 (1990).

40. Venyaminov, S. Y., and Kalnin, N. N., *Biopolymers* **30**, 1243 (1990).

41. Boulkanz, L., Vidal-Madjar C., Balcar, N., and Baron, M. H., *J. Colloid Interface Sci*. **188**, 58 (1997).

42. Arrondo, J. L. R., Muga, A., Castresana, J., and Goni, F. M., *Prog. Biophys. Molec. Biol*. **59**, 23 (1993).

43. Byler, D. M., and Susi, H., *J. Ind. Microbiol*. **3**, 73 (1988).

44. Byler, D. M., and Susi, H., *Biopolymers* **25**, 469 (1986).

45. Surewicz, W. K., and Mantsch, H. H., *Biochim. Biophys. Acta* **952**, 115 (1988).

46. Baron, M. H., de Loze, C., and Fillaux, F., *Biopolymers* **11**, 2063 (1972).

47. de Loze, C., Baron, M. H., and Fillaux, F., *J. de Chimie Physique* **75**, 632 (1978).

48. Casal, H. L., Köhler, U., and Mantsh H. H., *Biophys. Biochem. Acta* **957**, 11 (1988).

49. Jackson, M., and Mantsh H. H., *Biophys. Biochem. Acta* **1118**, 139 (1988).

50. Jackson, M., Haris, P. I., and Chapman, D., *Biochemistry* **30**, 9681 (1991).

51. Wetzel, R., Becker, M., Bahlke, J., Billwitz, H., Böhem, S., Ebert, B., Haman, H., Krumbiegel, and Lassman, G., *Eur. J. Biochem.* **104**, 469 (1980).

52. Heremans, L., and Heremans H., *Biophys. Biochem. Acta* **999**, 192 (1989).

53. Baron, M. H., de Loze, C., Mejean, T., Coulange, M. J., Turpin, P. Y., and Chinsky, L., *J. de Chimie Physique* **80**, 729 (1983).

54. Rawn, J., D., "Biochemisry" (Neil Paterson, Ed.) Carolina biological Supply Company, Burlington, 1989.

55. Blow, D., *Accoun. Chem. Res.* **9**, 145 (1976).

56. Henderson, R., *J. Mol. Biol.* **54**, 341 (1970).

57. Sigler, B. P., Blow, D. M., Mattews, B. W., and Henderson, R., *J. Mol. Biol.* **35**, 143 (1968).

58. Lee, C. S., and Belfort, G., *Pro. Natl. Acad. Sci.* **86**, 8392 (1989).

59. Norde, W., and Lyklema, J., .*J. Colloid Interface Sci.*; **66**, 257 (1978).

60. Haynes, C. A., and Norde, W., *Colloids Surf. B : Biointerfaces* **2**, 517 (1994).

61. Yoon, B. J., and Lenhoff, A. M., *J. Phys. Chem.* **96**, 3130 (1992).

62. Pantazaki, A., Baron, M. H., Revault, M., and Vidal-Majdar, C., *J. Colloid Interface Sci.* **207**, 324 (1998).

63. Baron, M. H., and Quiquampoix, H., *in* "Fifth International Conference on the Spectroscopy of Biological Molecules" (T. Theophanides, J. Anastassopoulo and N. Fotopoulos, Eds), p. 109. Kluwer Academic Publishers, Dordrecht, 1993.

64. Matumoto-Pintro, P. T., and Quiquampoix, H., *in* "Microbiologie Industrielle et Environnement" (B. Baleux, M. Demazeaud, C. Divies, F. Gendre and R. Moletta, Eds), p. 195. Société Française de Microbiologie, Paris, 1997.

65. Pistorius, A. M. A., *Spectrosc. Europe*, **7/4**, 8 (1995).

66. Heise, H. M., Marbach, R., Koschinsky, T. and Gries, F. A., *Applied Spectrosc*. **48**, 85 (1994).

Journal of Colloid and Interface Science 214 (1999) 319-332.
DOI : 10.1006/jcis.1999.6189

TABLES

Amide I′ component (cm^{-1})	Chymotrypsin domains	pD 4.5 (%)	pD 5.6 (%)	pD 7.5 (%)	pD 8.6 (%)	pD 11.6 (%)	pD 12.4 (%)
1690	Hydrophobic	2.9	0.5	0.0	0.0	0.0	0.0
1682	Hydrophobic	5.6	7.2	6.5	6.6	4.1	4.9
1670	Polar	11.8	11.7	11.7	11.2	11.4	11.1
1660	Polar	12.1	12.1	12.1	12.7	13.3	13.2
1651	Helix	16.6	16.5	16.8	15.1	14.5	13.1
1644	Hydrated random	8.3	7.1	7.4	11.6	18.5	18.7
1638	Unhydrated sheets	22.1	24.9	24.1	19.5	11.4	8.9
1630	Hydrated sheets	15.3	16.1	17.2	19.1	22.1	22.8
1618	Self-association	4.4	4.1	4.4	4.1	4.8	7.3

Table 1

pD dependent intensities of the Amide I components, expressed as percentage of the overall Amide intensity, for chymotrypsin in buffered dideuterium oxide solution.

Amide I′ component (cm^{-1})	Chymotrypsin domains	pD 4.5 (%)	pD 5.9 (%)	pD 7.7 (%)	pD 8.7 (%)	pD 11.8 (%)
1690	Hydrophobic	2.6	1.1	0.6	0.2	0.2
1682	Hydrophobic	6.2	7.8	6.9	5.4	5.0
1670	Polar	12.2	11.8	11.5	11.0	11.2
1660	Polar	12.5	13.4	13.4	12.9	13.1
1651	Helix	14.6	13.9	14.9	14.9	13.9
1644	Hydrated random	11.2	11.6	9.9	12.1	16.8
1638	Unhydrated sheets	15.5	15.5	18.9	16.2	9.9
1630	Hydrated sheets	17.3	17.5	17.1	18.3	22.2
1618	Self-association	7.3	7.6	6.7	8.7	7.5

Table 2

pD dependent intensities of the Amide I components, expressed in percentage of the overall Amide intensity, for chymotrypsin adsorbed on montmorillonite in buffered dideuterium oxide suspension.

Journal of Colloid and Interface Science 214 (1999) 319-332.
DOI : 10.1006/jcis.1999.6189

FIGURES AND FIGURE CAPTIONS

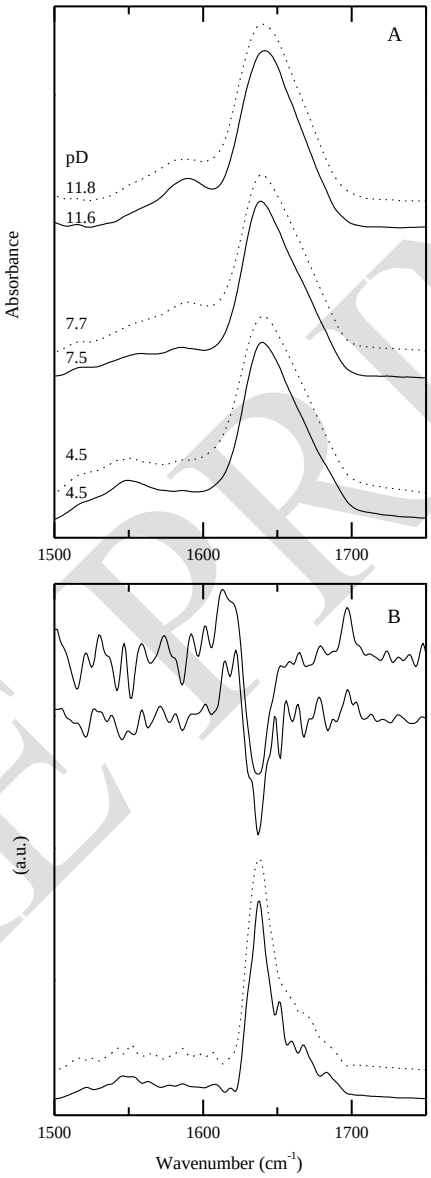

Journal of Colloid and Interface Science 214 (1999) 319-332.
DOI : 10.1006/jcis.1999.6189

Figure 1

Absorbance spectra (1500-1750 cm^{-1}) for chymotrypsin in solution, or adsorbed on montmorillonite in suspension, in buffered dideuterium oxide, for 3 pD ranges (A) ; second derivative and "curvature spectra" spectra for pD 4.5 (B). Solution (——), adsorbed state (-----).

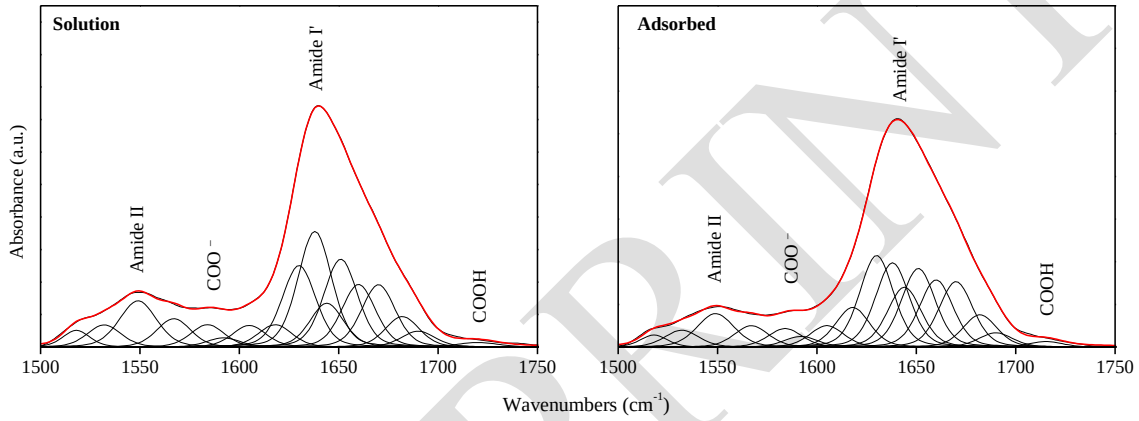

Figure 2

Computed decompositions of absorbance spectral profiles (1800-1500 cm^{-1}) for chymotrypsin in solution (A), or adsorbed on montmorillonite in suspension (B), in buffered dideuterium oxide at pD 4.5.

Journal of Colloid and Interface Science 214 (1999) 319-332.
DOI : 10.1006/jcis.1999.6189

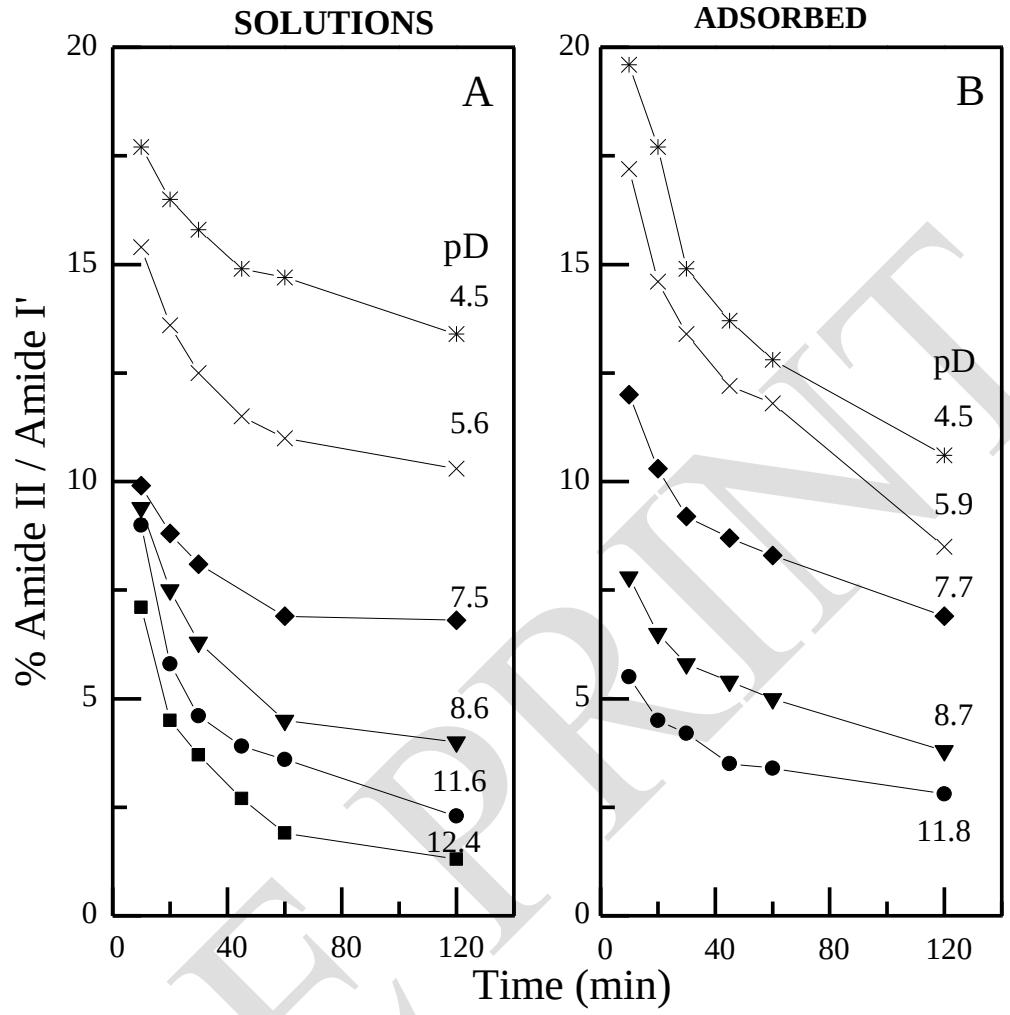

Figure 3

Time dependence of the Amide II intensity (% of the overall Amide I intensity) for chymotrypsin in solution (A), or adsorbed on montmorillonite in suspension (B), in buffered dideuterium oxyde at various pD.

Journal of Colloid and Interface Science 214 (1999) 319-332.
DOI : 10.1006/jcis.1999.6189

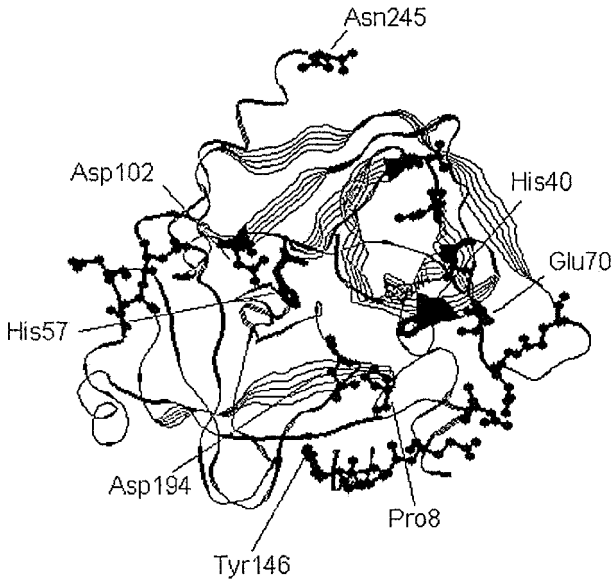

Figure 4

Structural representation of crystallized α-chymotrypsin (ref. PDB, 2CHA). Sticks schematize His-40 and -57 residues. Balls and sticks schematize: all Asp and Glu carboxylic (carboxylate) residues (only internal Asp-102, -194, and Glu-70 are explicitly numbered), Tyr-146 residue, Asn-245 carboxylic (carboxylate) end chain and Pro-8 residue. Location of Val-9—Leu-13 carboxylic (carboxylate) end chain segment is not provided in the X-ray 3 dimensional structure (31).

Journal of Colloid and Interface Science 214 (1999) 319-332.
DOI : 10.1006/jcis.1999.6189

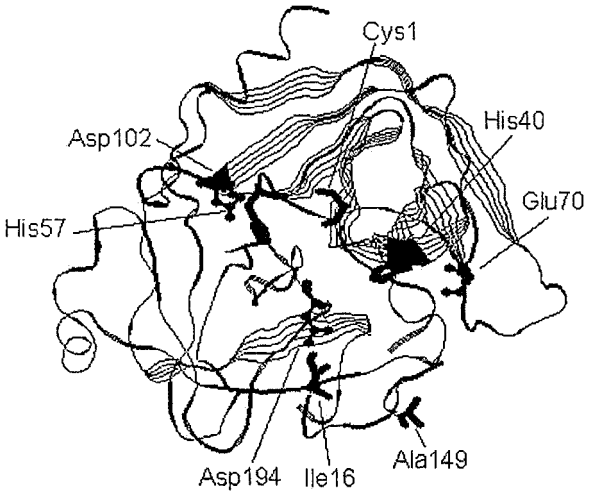

Figure 5

Structural representation of crystallized α-chymotrypsin (ref. PDB, 2CHA). Sticks schematize His-40 and -57 residues, Cys-1, Ile-16 and Ala-149 amino (aminium) end chain. Balls and sticks represent the 3 internal carboxylic (carboxylate) residues: Asp-102, -194 and Glu-70.

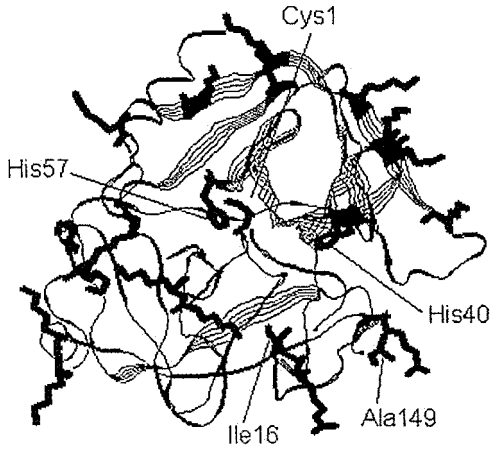

Figure 6

Structural representation of crystallized α-chymotrypsin (ref. PDB, 2CHA). Sticks schematize all His, Lys and Arg (amino/imino or aminium/iminium) residues and the 3 amino/aminium end chain: Cys-1, Ile-16 and Ala-149.

Journal of Colloid and Interface Science 214 (1999) 319-332.
DOI : 10.1006/jcis.1999.6189

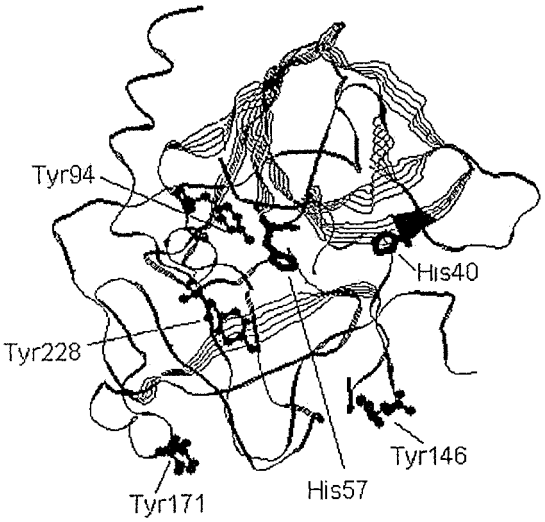

Figure 7

Structural representation of crystallized α-chymotrypsin (ref. PDB, 2CHA). Sticks schematize His-40 and -57 residues ; balls and sticks the 4 Tyr residues.

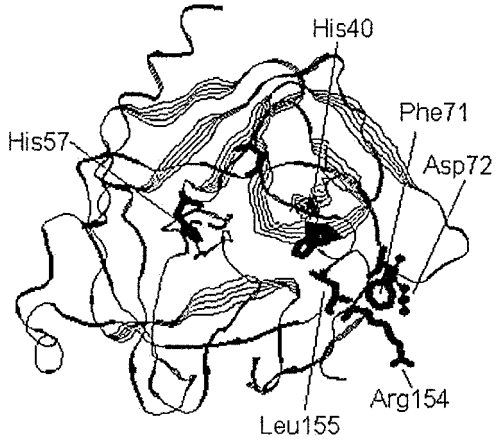

Figure 8

Structural representation of crystallized α-chymotrypsin (ref. PDB, 2CHA). Sticks schematize His-40 and -57, Arg-154 and Leu-155 residues ; balls and sticks Asp-72 and Phe-71 residues.

Journal of Colloid and Interface Science 214 (1999) 319-332.
DOI : 10.1006/jcis.1999.6189

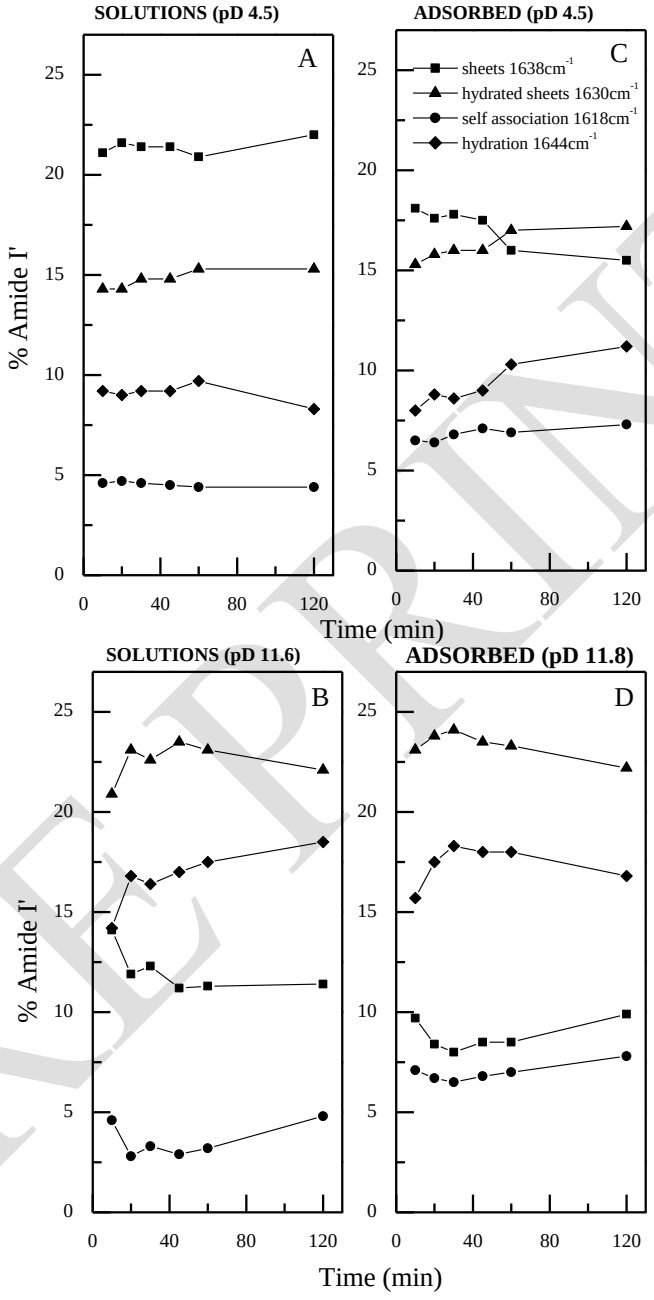

Figure 9

Journal of Colloid and Interface Science 214 (1999) 319-332.
DOI : 10.1006/jcis.1999.6189

Time dependent Amide I components (%) for α-chymotrypsin in solution, pD 4.5 (A), pD 11.5 (B), or adsorbed on montmorillonite in suspension, pD 4.5 (C), pD 11.8 (D), in buffered dideuterium oxide.

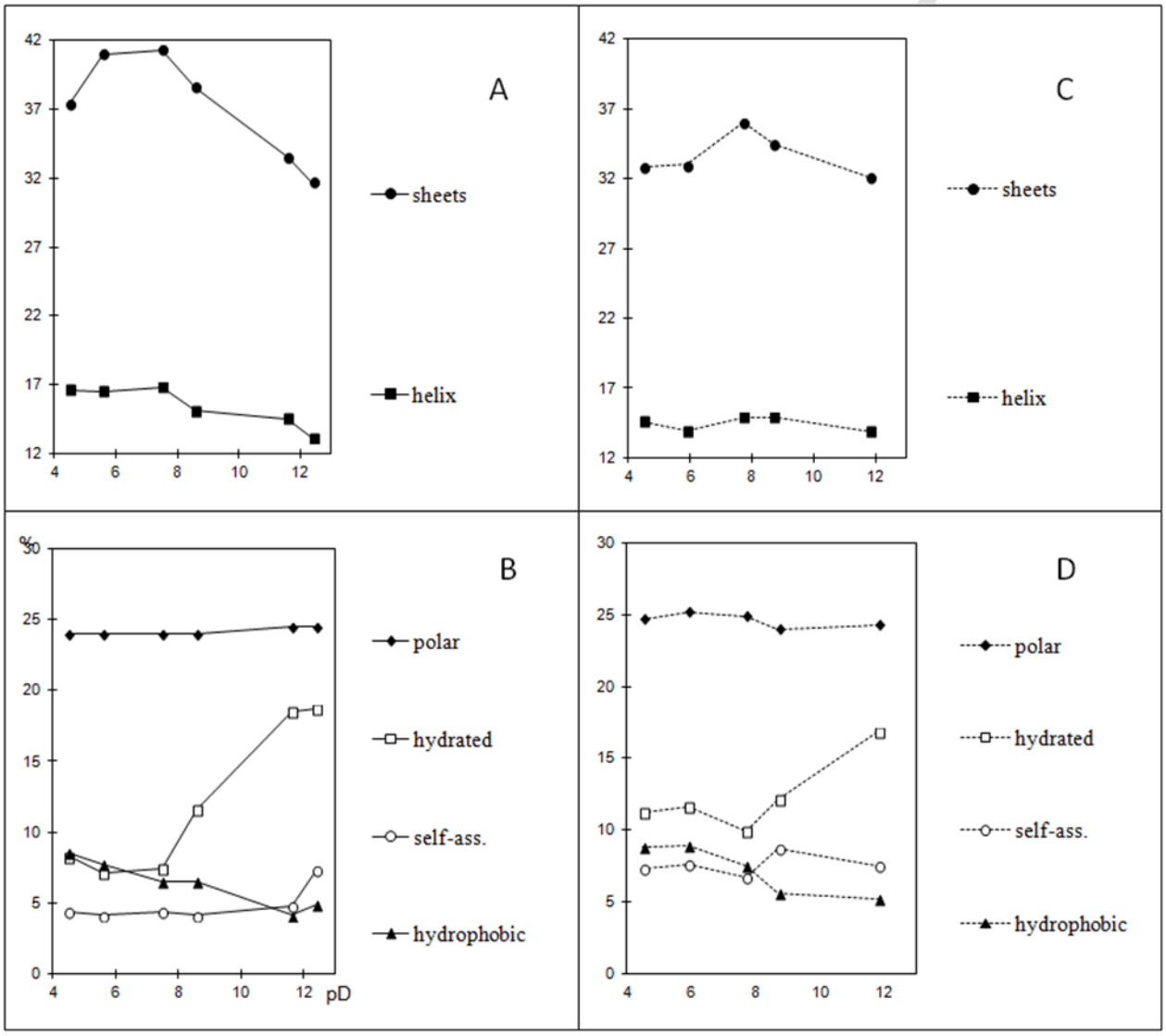

Figure 10

pD dependent Amide I components (%) for α-chymotrypsin in solution (A, B), or adsorbed on montmorillonite in suspension (C, D), in buffered dideuterium oxide (2 h). Secondary structures

Journal of Colloid and Interface Science 214 (1999) 319-332.
DOI : 10.1006/jcis.1999.6189

(A, C): for β-sheets the contribution of hydrated and unhydrated domains (Tables 1, 2) are added.

Differentiate solvated domains (B, D).

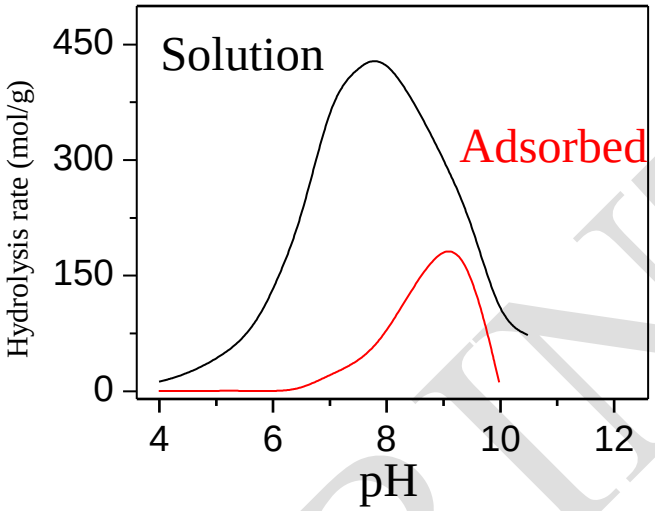

Figure 11

pH dependent hydrolysis of BTNA with α-chymotrypsin in solution, or with α-chymotrypsin adsorbed on montmorillonite in suspension

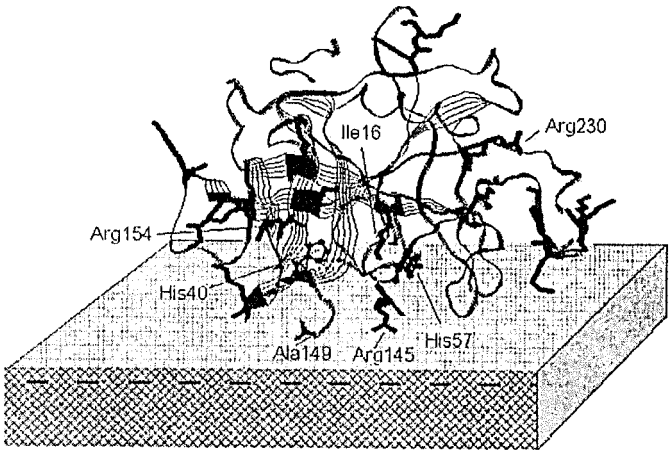

Figure 12

Journal of Colloid and Interface Science 214 (1999) 319-332.
DOI : 10.1006/jcis.1999.6189

Schematic representation of an orientation for α-chymotrypsin (ref. PDB, 2CHA) adsorbed on montmorillonite below pH 7 via His^+, Lys^+, Arg^+ side chains and Ala^+-149 aminium end chain (pH<7). Green ball and sticks schematize His residues; yellow sticks Lys and Arg, Ile-16 and Ala-149 aminium end chains. Only His and Arg residues and Ile-16 and Ala-149 aminium end chains are explicitly numbered.

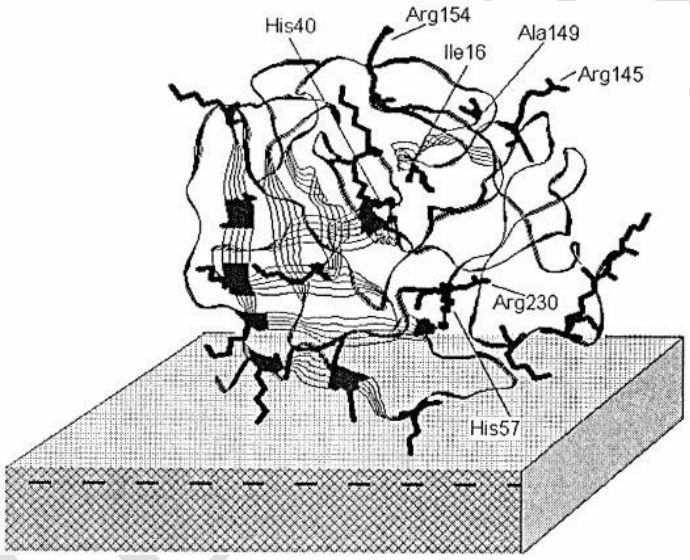

Figure 13

Schematic representation of an orientation for α-chymotrypsin (ref. PDB, 2CHA) adsorbed on montmorillonite above pH 8 only via Lys^+ side chains. Green ball and sticks schematize His residues; yellow sticks Lys and Arg residues and Ile-16 and Ala-149 amine end chains.